



NUMERICAL STUDY OF THE FLOW FIELD FOR MODERATE-SLOPE STEPPED SPILLWAYS

ETUDE NUMERIQUE DU CHAMP D'ÉCOULEMENT DANS LES CANAUX EN MARCHÉ D'ESCALIER À PENTE MOYENNE

BENTALHA C., HABI M.

Department of Hydraulic Engineering, Abou Bakr Belkaid University,
Tlemcen, Algeria

c_bentalha@yahoo.fr

ABSTRACT

Today several dams are equipped by the stepped spillways because of efficient for energy dissipation and of high contribution to the stability of these structures. The air-water flow on stepped spillway can prevent or reduce the cavitation damage. The air entrainment starts where the boundary layer attain the free surface of flow; this point is called “point of inception”. The objective of this paper is to study the characteristics of flow at stepped spillways such as velocity profile, pressure field and effect of step height in risk of cavitation by numerical method. In this research, the Ansys fluent computational fluid dynamics (CFD) is used to simulate water flow down stepped spillway and turbulence parameters are calculated by standard $k-\varepsilon$ model. The volume of fluid (VOF) model is utilised to track free surface of flow. The found numerical results agree well with experimental results.

Keywords: inception point, flow field, Ansys Fluent, VOF Model, Stepped Spillway, Standard $k-\varepsilon$ Model.

RÉSUMÉ

Aujourd'hui, plusieurs barrages sont équipés par des déversoirs en escaliers en raison de leur efficacité à la dissipation d'énergie et de leur contribution importante à la stabilité de ces structures. L'écoulement air-eau sur les canaux en marche escalier peut prévenir ou réduire les dommages causés par la cavitation. L'entraînement d'air commence lorsque la couche limite atteint la surface libre de l'écoulement; ce point est appelé «point d'inception». L'objectif de cet article est d'étudier les caractéristiques d'écoulement sur un coursier en marche escalier, telles que le profil de vitesse, le champ de pression et l'effet de la hauteur du marche sur le risque de cavitation par méthode numérique. Dans cette recherche, le logiciel Ansys Fluent (CFD) est utilisée pour simuler l'écoulement de l'eau dans un déversoir en marche escalier et les paramètres de turbulence sont calculés à l'aide du modèle standard $k-\varepsilon$. Le modèle de volume de fluide (VOF) est utilisé pour suivre la surface libre de l'écoulement. Les résultats numériques trouvés concordent bien avec les résultats expérimentaux.

Mots clés : point d'inception, champ d'écoulement, Ansys FLUENT, méthode VOF, marche escalier, modèle ($k-\varepsilon$),

INTRODUCTION

Evacuating the surplus of water by smooth spillway from the dam to stalling basin creates high levels of kinetic energy. The amount of kinetic energy can be reduced by building of series of steps on the surface of spillway (Chanson, 2001). Chinnarasri et al (2012) showed from experiment that, the energy dissipation increased when the number of steps increased for the case of skimming flow. Rice and Kadavy (1996), found from experiments on a specific model study of a stepped spillway on a 2.5(H):1(V) slope that the energy dissipated with steps was two to three times as great as the energy dissipated with a smooth surface, the studies of Rajaratman (1990) and Christodoulou (1993) demonstrated also effectiveness the stepped chute for dissipation of kinetic energy, thereby reducing the required size of the stilling basin at the toe of the dam. Stepped chute flows are characterised by a high level of turbulence, and large amounts of air which can prevent or reduce the cavitation erosion damage.

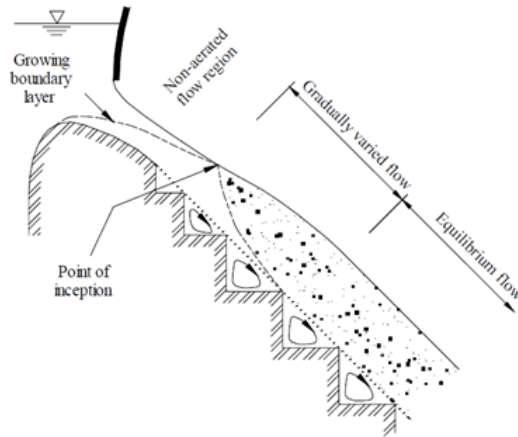


Figure 1: Position of the inception point in stepped spillway

The flows on stepped spillways can be divided into different flow regimes, i.e. nappe flow, transition flow and skimming flow regimes with increasing discharge (Chanson 1994). The changes between flow regimes depend on the spillway configuration including the channel slope, the step height and the discharge. In the skimming flow regime, air entrainment occurs when the turbulent boundary layer thickness coincides with the water depth (Chanson 1997). This location is called the inception point (e.g. Figure 1). At the inception point upstream, the flow is smooth and glassy whereas at the downstream of the inception point the flow becomes uniform as the depth of the air-water mixture grows.

Historically, most experimental research has been developed to characterise the flow over stepped spillway. Today, with the development of computational fluid dynamics (CFD) branch, flow over stepped spillway can be simulated to validate experimental results and to help in the design of stepped spillway together with the physical model (Chen et al 2002; Bombardelli et al 2011; Mohammed et al. 2012; Bentalha and Habi 2015; Afshin and Mitra 2012; Cheng et al 2006, Bentalha and Habi, 2017).

This study, present the results of numerical simulation flow in moderate slope stepped spillway obtained by using Ansys Fluent computational fluid dynamics (2014) to show the distribution of velocity and pressure along the stepped spillway. Likewise the cavitation damage has been discussed in this work. The simulation results were compared with the experimental data of Felder and Chanson (2009) and Chanson, H. and Toombes, L. (2001).

NUMERICAL MODEL

Ansys Fluent computational fluid dynamics (CFD) is used to solve Navier-Stokes equations that are based on momentum and mass conservation of multi-phase flow over stepped spillway. Because the standard $k - \varepsilon$ model is still a good tool for numerical simulation of flow in stepped spillways and verified by experimental and field data (Chen et al 2002), it is used to simulate turbulence.

Continuity equation:

$$\frac{\partial \rho}{\partial t} + \frac{\partial \rho u_i}{\partial x_i} = 0 \quad (1)$$

Momentum equation:

$$\frac{\partial \rho u_i}{\partial t} + \frac{\partial}{\partial x_j} (\rho u_i u_j) = -\frac{\partial p}{\partial x_i} + \rho g_i + \frac{\partial}{\partial x_j} \left\{ \left(\mu + \mu_t \right) \left(\frac{\partial u_i}{\partial x_j} + \frac{\partial u_j}{\partial x_i} \right) \right\} \quad (2)$$

Turbulence kinetic energy equation (k):

$$\frac{\partial}{\partial t} (\rho k) + \frac{\partial}{\partial x_i} (\rho k u_i) = \frac{\partial}{\partial x_j} \left[\left(\mu + \frac{\mu_t}{\sigma_k} \right) \frac{\partial k}{\partial x_i} \right] + G_k - \rho \varepsilon \quad (3)$$

Turbulence dissipation rate energy equation (ε):

$$\frac{\partial}{\partial t} (\rho \varepsilon) + \frac{\partial}{\partial x_i} (\rho \varepsilon u_i) = \frac{\partial}{\partial x_j} \left[\left(\mu + \frac{\mu_t}{\sigma_\varepsilon} \right) \frac{\partial \varepsilon}{\partial x_i} \right] + C_{\varepsilon 1} \frac{\varepsilon}{k} G_k - C_{\varepsilon 2} \rho \frac{\varepsilon^2}{k} \quad (4)$$

Where, G_k is production of turbulent kinetic energy which can be given as

$$G_k = \mu_t \left(\frac{\partial u_i}{\partial x_j} + \frac{\partial u_j}{\partial x_i} \right) \frac{\partial u_i}{\partial x_j} \quad (5)$$

μ_t is the turbulent viscosity that satisfies

$$\mu_t = \rho C_\mu \frac{k^2}{\varepsilon} \quad (6)$$

$C_\mu=0.09$ is a constant determined experimentally;

σ_k and σ_ε are turbulence Prandtl numbers for k and ε equation respectively,

$\sigma_k=1.0$, $\sigma_\varepsilon=1.3$,

$C_{1\varepsilon}$ and $C_{2\varepsilon}$ are ε equation constants, $C_{1\varepsilon}=1.44$, $C_{2\varepsilon}=1.92$.

The volume of fluid (VOF) method is applied to simulate the free surface between water and air (Ansys Fluent 2014). In this approach, the tracking interface between air and water is accomplished by the solution of a continuity equation for the volume fraction of water:

$$\frac{\partial \alpha_w}{\partial t} + \frac{\partial \alpha_w u_i}{\partial x_i} = 0 ; 0 \leq \alpha_w \leq 1 \quad (7)$$

Where, α_w is volume fraction of water.

In each cell, the sum of the volume fractions of air and water is unity. So, volume fractions of air denote α_a can be given as

$$\alpha_a = 1 - \alpha_w \quad (8)$$

The volume fraction, momentum and turbulence closure equations were discretised by employing a conservative, second-order accurate upwind scheme. The pressure-velocity coupling algorithm is the pressure-implicit with splitting of operators (PISO). The boundary conditions in this study are velocity inlet as water inlet and air inlet, outlet as a pressure outlet type. All of the walls as a stationary, no-slip wall. The viscosity layer near to the wall dealt with the standard wall function (see figure 2). The boundary conditions for the turbulent quantities such as k and ε can be calculated from (Ansys Fluent 2014):

$$k = \frac{3}{2} (U_{avg} I)^2 \quad (9)$$

$$\varepsilon = C_u^{3/4} \frac{k^{3/2}}{0.07 D_H} \quad (10)$$

Where, I is turbulence intensity can be estimated from the following formula derived from an empirical correlation for pipe flows:

$$I = 0.16 (Re_{D_H})^{-1/8} \quad (11)$$

U_{avg} is the mean velocity of water flow inlet and D_H is the hydraulic diameter.

Two physical model provided by Felder and Chanson (2009) and Chanson and Toombes. (2001) are simulated by Ansys Fluent. The experiments of Felder and Chanson (2009) and Chanson and Toombes (2001) were conducted in a same channel with 3.2 m long and 1 m wide and channel slope is $21,8^\circ$, but two different step heights were investigated.

The stepped spillway used by Chanson and Toombes (2001) (see figure 2) contains nine identical steps (height = 0.1 m, length = 0.25 m) and the stepped spillway used by Felder and Chanson (2009) contains 20 identical steps with 0.05m height and 0.125 m length by step. The two-dimensional numerical domain was divided into unstructured grids (triangular cell) that had a high adaptability to the complex geometry and boundary. Triangular meshes with 0.015 m^2 are used.

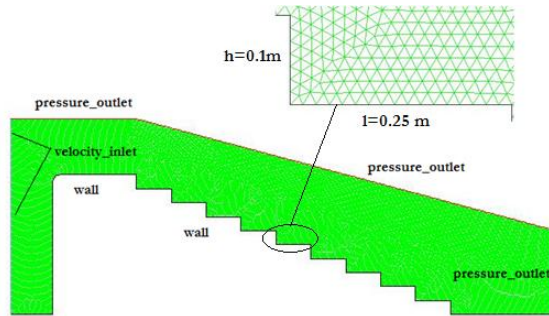


Figure 2: Boundary conditions and numerical model of a stepped spillway

RESULTS AND DISCUSSIONS

Figure 3 shows the transition flow and skimming flow simulated by VOF model and obtained by experiments (Chanson and Toombes 2001). This figure shows good agreements between the numerical results and experimental results. From this figure, the transition flow observed for the low range of water discharge and the skimming flow occurred for upper range of water discharge. In skimming flows, the water skimmed smoothly over the pseudo bottom formed by the steps.

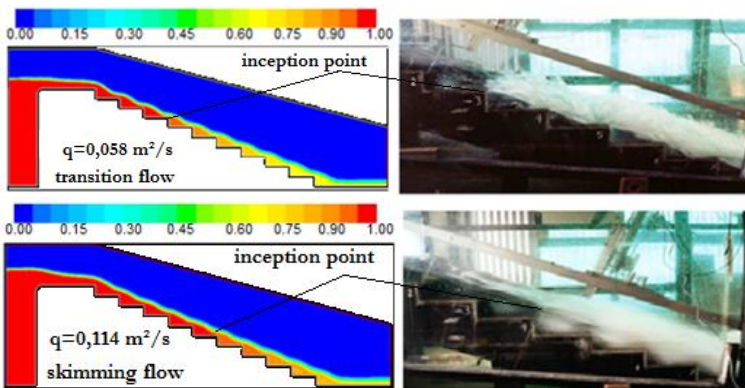


Figure 3: Transition flow and skimming flow simulated by VOF model and obtained by experiments

In transition flows, the water exhibited a chaotic behaviour associated with the intensive recirculation in cavities, strong spray and splashing. Furthermore the skimming flow observed by Felder and Chanson (2009) correspond with predict by fluent (see figure 4). From figure 4 the skimming flow was appeared for

$q=0,043 \text{ m}^2/\text{s}$ but in figure 3 the transition flow was observed for flow rate greater than $0,043 \text{ m}^2$, this remark demonstrate the effect of step height on the onset of skimming flow. Chanson (1994) proposed the equation for the onset of skimming flow for spillway slopes range from 11.3° to 38.7° as follows:

$$\frac{d_c}{h} > 1.057 - 0.465 \frac{h}{l} \quad (12)$$

were,

d_c = critical flow depth, for rectangular channel $d_c = \sqrt[3]{q^2/g}$, h =step height and l =step length

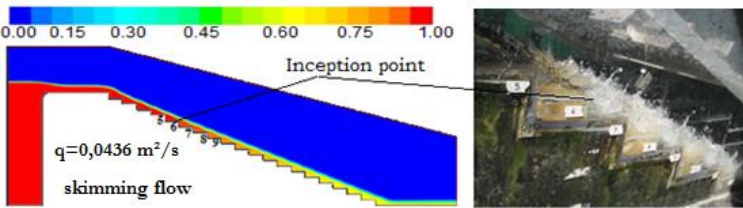


Figure 4: Skimming flow obtained by experiment and simulation

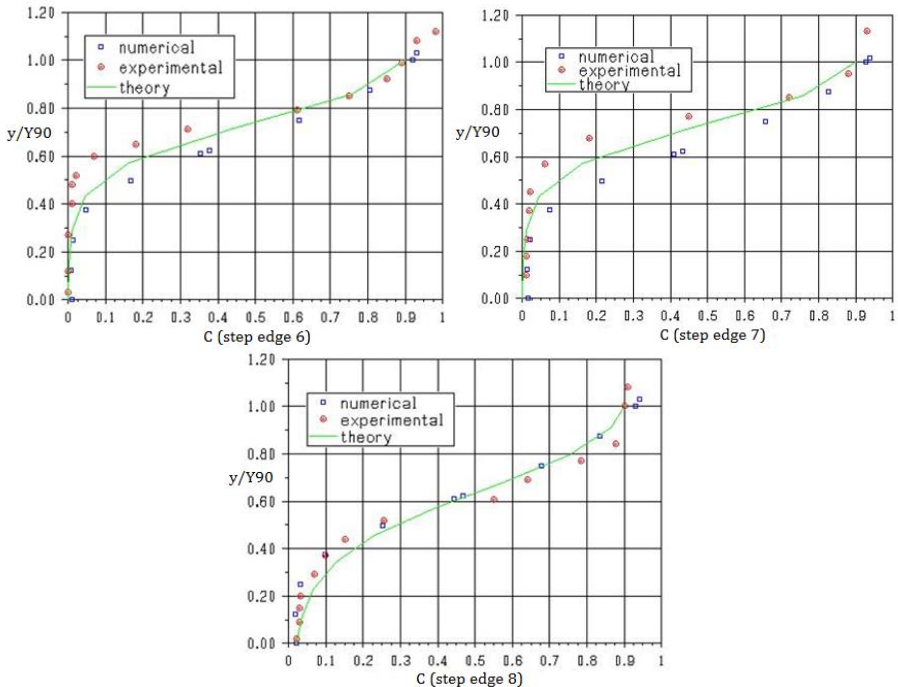


Figure 5: Experimental and computational air concentration distribution compared with equation (13)

The start of air entrainment is defined by the point where the boundary layer thickness reaches the water depth, figure 3 and 4 present also a good accordance between the positions of inception point obtained by experiment and by simulation.

Downstream of the inception point of free-surface aeration, air and water are fully mixed, forming a homogeneous two-phase flow. In skimming flow, the air concentration distribution may be described by an analytical solution of the air bubble advective diffusion equation:

$$C = 1 - \tanh^2 \left(K'' - \frac{y}{2D_0} + \frac{\left(\frac{y}{Y_{90}} - \frac{1}{3}\right)^3}{3D_0} \right) \quad (13)$$

where y is distance measured normal to the pseudo-invert, Y_{90} is the characteristic distance where $C = 90\%$, K is an integration constant and D_0 is a function of the of the mean air concentration C_{mean} (Chanson, 2001). In figure 5, the computed air concentration profiles downstream of the inception point is compared with experimental data Chanson H. and Toombes L. (2001) and with equation (13) at different locations for discharge of $0.182 \text{ (m}^2/\text{s)}$.

As can be seen, there are little differences between the numerical and experimental results because the VOF model underestimate the value of air concentration (Afshin and Mitra 2012). Equation 13 compares favourably with the numerical and experimental air concentration profiles.

The air-water velocity profile at step edge is presented in figure 6 for $q=0,182 \text{ m}^2/\text{s}$. The percentage difference between numerical and experimental data was less than 13%. In the skimming flow, the velocity profile increase from the pseudo bottom at the free surface flow.

Based on previous study's (Chanson 2001, Hunt and Kadavy 2010), the distribution of air-water velocity follows a power law given by:

$$\frac{v}{V_{90}} = \left(\frac{y}{Y_{90}} \right)^{1/n} \quad (14)$$

Where V_{90} is the characteristic velocity for $C = 90\%$. The exponent n is obtained from experiments data. Chanson and Toombes (2001) found $n = 5.1$ and 6 for y/h values of 1.5 and 1.1 , respectively. Hunt and Kadavy (2010) taken $n=6.0$ with slope 14° . Matos (in Chanson and Toombes 2001) obtained $n = 4$. Felder and Chanson (2009) proposed $n=10$ for $y/Y_{90} < 1$. This figure showed that the velocity profiles follow a power law distribution with $n=6.0$ and $n=5.1$ downstream of the inception point.

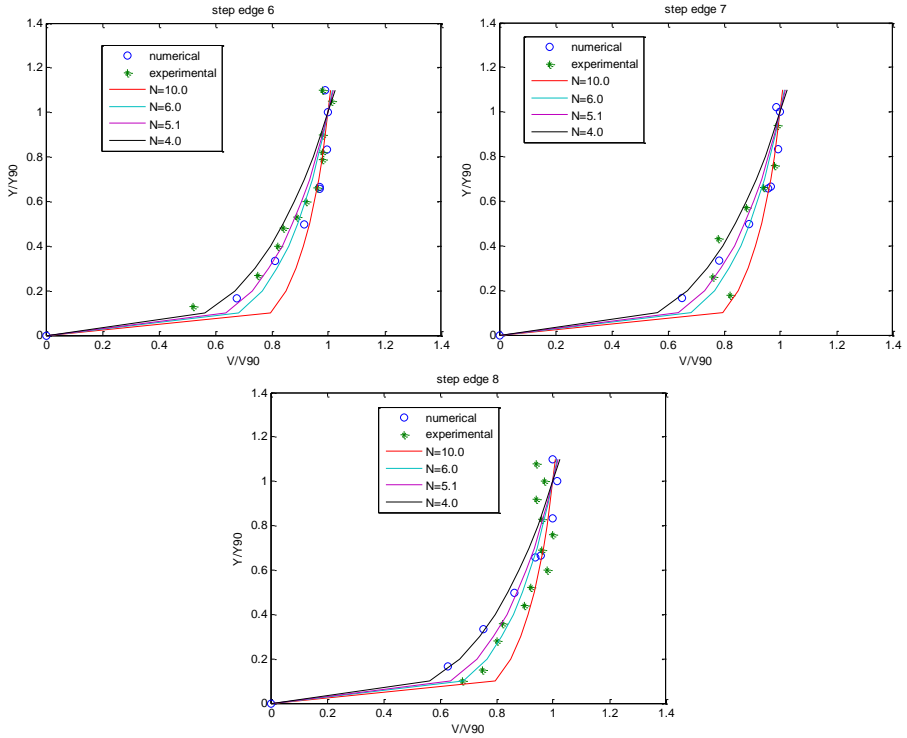


Figure 6: Comparison of the power law with a Velocity obtained by simulation and measurement in Chanson and Toombes 2001, for $q=0,128 \text{ m}^2/\text{s}$

In order to evaluate the risk of cavitation in stepped channel; figure 7 and figure 8 show the contour of pressure for step height equal 0.1 and 0.05 respectively. According to these figures, the maximum value of negative pressure is appeared in the stepped spillway with step height $h=0.1 \text{ m}$, is due by separation flow between skimming flow and the eddy in this region.

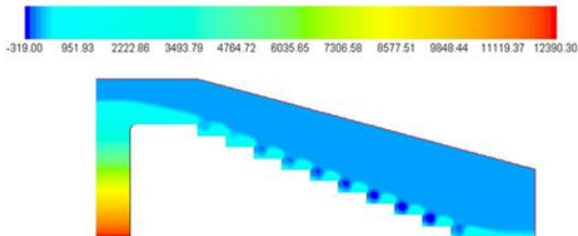


Figure 7: Contour of static pressure along the stepped spillway with $h=0.1 \text{ m}$ for $q=0.122 \text{ m}^2/\text{s}$

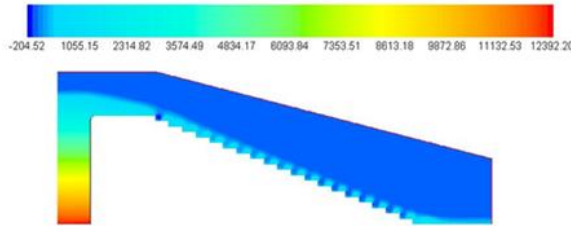


Figure 8: Contour of static pressure along the stepped spillway with $h=0.05$ m for $q=0.122\text{m}^2/\text{s}$

The risk of cavitations appears for high velocity flows and when the values of static pressure becomes lower than vapour pressure of water, resulting in the local cavitation index:

$$\sigma = \frac{P - P_V}{\frac{\rho V^2}{2}} \quad (15)$$

Where V is reference flow velocity, P is reference flow pressure, P_V is water vapour pressure and ρ is water density. To prevent the cavitation damage to a stepped spillway, it is required to keep σ more than cavitation inception index σ_i . Based on the study of Falvey (1990), the cavitation inception index varies between 0.076 and 1,2 for all surfaces roughness. Matos et al (2014) proposed formulae to evaluate the damage of cavitations at the inception point:

$$\sigma = 0.064 F_*^{-0.23} \left[1 + \frac{4.762 \left(\frac{P_{atm} - P_V}{\rho g} \right)}{k_s F_*^{0.59}} \right] \quad (16)$$

Where:

$$k_s = h \cos \theta$$

h = step height

θ = channel slope

F_* = Froude number defined in terms of the roughness height:

$$F_* = q / [g(\sin \theta) \{k_s\}^3]^{0.5}$$

q = unit discharge

g = gravitational constant

In figure 10, equation 16 is plotted as function F_* for step height equal 0.05 m and 0.1m. This figure shows that, the risk of cavitation increase with increasing of F_* therefore when the flow rate increase, also with growing of step height .

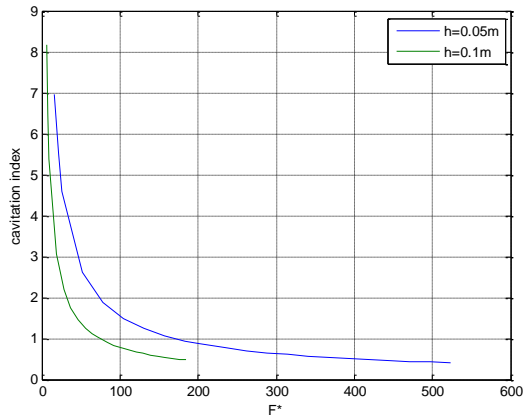


Figure 9: Cavitation index versus Froude surface roughness, F_*

CONCLUSION

The software Ansys Fluent was used to simulate air-water flow along stepped spillways. Free surface of water was tracked by VOF model and turbulence flow was estimated by $k-\epsilon$ Standard Model. The experimental studies of Chanson and Toombes (2001) and of Felder and Chanson (2009) are used to validate the numerical results of aerated flow over the stepped spillway. It was found that the calculated inception point is well agreed with that of measurement and the air concentration distribution may be described by an analytical solution of the air bubble advective diffusion equation. It has been verified that the velocity profile follows power law distribution with exponent $n=6$ and $n=5.1$. The maximum value of negative pressure is appeared in the stepped spillway with step height $h=0.1$ m, is due by separation flow between skimming flow and the eddy in this region. Finally the risk of cavitation damage increase by increasing of flow rates and step height.

REFERENCES

- ANSYS Inc. (2014). ANSYS Fluent Version 15.0 User's Guide.
- AFSHIN E., MITRA J. (2012). Comparison of Mixture and VOF Models for Numerical Simulation of Air-entrainment in Skimming Flow over Stepped Spillways .Journal of Science Direct. Procedia engineering Vol.28, pp 657 – 66.

- BENABDESSELAM A., ACHOUR B., HOUICHI L. (2017). Hydraulic jumps in a straight rectangular compound channel: Theoretical approach and experimental study, *Larhyss Journal*, n° 29, pp. 323-340.
- BENTALHA C., HABI M. (2015). Numerical Simulation of Air Entrainment for Flat-sloped Stepped Spillway , *The Journal of Computational Multiphase Flows*, Vol. 7, n°1, pp. 33-41.
- BENTALHA C., HABI M. (2017). Numerical simulation of water flow along stepped spillways with non uniform step heights, *Larhyss Journal*, n°31, pp. 115-129.
- BERREKSI A., BENMAMAR S., KETTAB A., REMINI B., IKNI T., NAKIB M. (2016). Calcul numérique d'un écoulement bidimensionnel non permanent à travers un élargissement rectiligne symétrique à surface libre, *Larhyss Journal*, n°28, pp. 275-283.
- BOMBARDELLI F.A., MEIRELES I., MATOS J. (2010). Laboratory measurements and multi-block numerical simulations of the mean flow and turbulence in the non-aerated skimming flow region of steep stepped spillways. *Environmental Fluid Mechanics*. Vol. 11. issue .3 pp.263-288.
- BOUDJELAL S., FOURAR A., MERROUCHI F. (2015). Modélisation en 2D des écoulements brusquement instationnaires dans un canal prismatique à surface libre, *Larhyss Journal*, n°22, pp. 7-13.
- CHANSON H. (1994). Hydraulics of skimming flows over stepped channels and spillways. *IAHR, Journal of Hydraulic Research*. Vol 32, n°3, pp. 445-460.
- CHANSON H. (1997). *Air Bubble Entrainment in Free-Surface Turbulent Shear Flows*. Academic Press, London, UK, 401 pages ISBN 0-12-168110-6.
- CHANSON H. (2001). *The Hydraulics of Stepped Chutes and Spillways*. Balkema Publisher., Rotterdam, The Netherlands. ISBN 90 5809 352 2, 384 p.
- CHANSON H., TOOMBES L. (2001). *Experimental Investigations of Air Entrainment in Transition and Skimming Flows down a Stepped Chute. Application to Embankment Overflow Stepped Spillways*. Research Report n°.CE158, Department of Civil Engineering., University of Queensland, Brisbane, Australia, July.
- CHARLES E.RICE., KEM C.KADAVY. (1996). Model of A roller compacted concrete stepped spillway. *Journal of Hydraulic Engineering, ASCE*, Vol 122,n°6, pp.292-297.
- CHENG XIANGJU, CHEN YONGCAN, LUO LIN. (2006). Numerical simulation of air-water two-phase flow over stepped spillways. *Science in China Series E, Technological Sciences*, Vol 49, n°6, pp.674-684

- CHEN Q., DAI G.Q., LIU. H.W. (2002). Volume of Fluid Model for Turbulence Numerical Simulation of Stepped Spillway Over Flow. Journal of Hydraulic Engineering, ASCE Vol 128, n°7, pp. 683-688.
- CHINNARASRI C., KOSITGITTIWONG K. JULIEN. PY.(2012). Model of flow over spillways by computational fluid dynamics. Proceedings of the Institution of Civil Engineers, Vol. 167 ,n° 3, pp. 164-175
- CHRISTODOULOU G.C. (1993). Energy dissipation on stepped spillways. Journal of Hydraulic Engineering, ASCE Vol 119, n°5 ,pp. 644-650.
- FALVEY H. T. (1990). Cavitation in chutes and Spillways. Engineering monograph. n°42, United States Department of the Interior – Bureau of Reclamation, Denver, Colorado.
- HUNT SL., KADAVY KC. (2010). Energy dissipation on flat-sloped stepped spillways: part 2. downstream of the inception point. Transactions of the ASABE. Vol. 53, n°1, pp 111-118
- MOHAMMAD S, JALAL. A., Michael. P. (2012). Numerical Computation of Inception Point Location for Steeply Sloping Stepped Spillways. 9th International Congress on Civil Engineering, Isfahan University of Technology (IUT), May 8-10, Isfahan, Iran
- MATOS J., MEIRELES I. (2014). Hydraulics of stepped weirs and dam spillways: engineering challenges, labyrinths of research. 5th International Symposium on Hydraulic Structures, Brisbane, Australia. June 25-27.
- NEBBAR M.L., ACHOUR B. (2018). Design of rectangular channel at critical flow, Larhyss Journal, n° 34, pp. 7-20.
- RAJARATNAM N. (1990). Skimming flow in stepped spillways. Journal of Hydraulic Engineering, ASCE Vol 116, n°4, pp.587-591.
- FELDER S., CHANSON H. (2009). Energy dissipation, flow resistance and gas-liquid interfacial area in skimming flows on moderate-slope stepped spillways” Environmental Fluid Mechanics, Vol 9, n°4, pp. 427–441